Journal Applied Mechanics and Technical Physics, Vol. 37, No. 1, 1996

NUMERICAL SIMULATION AND EXPERIMENTAL INVESTIGATION OF ELECTROMAGNETIC ACCELERATION OF MICROPARTICLES USING A METAL ARMATURE

A. V. Plekhanov, A. N. Tereschenko, and D. V. Khandryga

UDC 620.193.1; 629.036.72

Acceleration of macroparticles in an electromagnetic railgun using a metal armature is preferable for a number of reasons. The main reasons, in our opinion, are: 1) the possibility to effectively accelerate heavy macroparticles (mass from hundreds of grams to several kilograms), 2) small voltage drop across the contact rail/armature, 3) longer accelerator life in comparison to that in the case of a plasma armature.

However, in this case many phenomena arise, whose physical nature is not yet clearly understood. Specifically, it is unknown what pressure along the sliding rail/armature contact would be sufficient to ensure good electrical contact, or how particle deformation influences the acceleration dynamics, etc.

It was studied numerically in [1] how the properties of armature material influenced acceleration dynamics in a railgun with copper rails; the following armature materials were studied: Al, Cu, W, and Mo. Preliminary investigations have shown that the acceleration was greatly influenced by particle construction, and (to a lesser extent) by properties of the armature material.

In [2] a simplified analysis was given as to how strained macrobody deformation affects the process of acceleration in a railgun. An analytical formula has been obtained for the coefficient which reduces the Lorentz force due to deformation with a corresponding increase in friction force.

In this paper the finite-element method was applied to the study of one of the factors influencing the friction force at high-velocity sliding contact, namely, the total normal pressure force which presses the armature to the surface of a railgun bore. The friction force is proportional to the normal pressure. Reducing the latter reduces the frictional losses, thus raising the electromagnetic projection efficiency. The main computed results are confirmed by experimental data.

1. Let us consider the factors influencing the level of normal pressure forces, using as an example a cylindrical armature (Fig. 1) moving in a round bore. Note that in this case contact between the armature and the bore occurs over some cylindrical surface of radius r_0 and the normal pressure force is given by

$$N = r_0 \int_0^{2\pi} \int_0^L p(\psi, z)\, d\psi\, dz, \tag{1.1}$$

where ψ, z are the cylindrical coordinates; p is the pressure upon the contact surface (contact pressure); L is the length of the generatrix of the cylindrical contact surface.

From (1.1) it follows that in order to reduce the total normal pressure force (and thus frictional losses) it is necessary to reduce the values of L and p or to achieve values such that the total normal pressure force N would be minimized.

The contact pressure at different parts of the contact surface has various physical natures. In the section with electric contact between rails and armature the contact pressure consists of the active pressure p_a, caused by electromagnetic forces, and the passive pressure p_p, due to total lateral deformation of the

Lyubertsy Scientific and Production Association "Soyuz," Dzerzhinsky 140056, Moscow Region.
Translated from Prikladnaya Mekhanika i Tekhnicheskaya Fizika, Vol. 37, No. 1, pp. 21–27, January–February, 1996. Original article submitted December 30, 1994.

0021-8944/96/3701-0017 $15.00

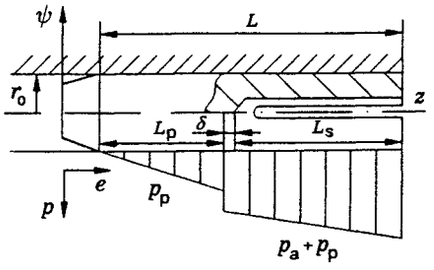

Fig. 1

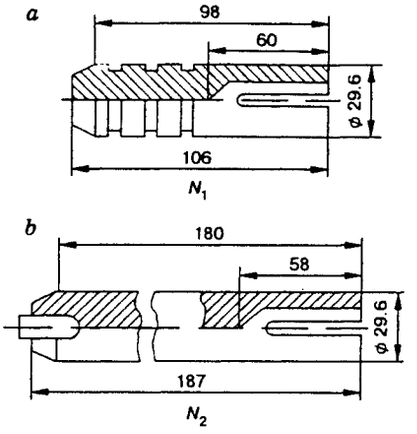

Fig. 2

armature and bore because of inertia and insertion forces. It is clear that the active pressure is necessary for ensuring good electric sliding contact. Therefore, shortening this part (hereinafter referred to as the active part) and decreasing the contact pressure there may lead not to a decrease of energy loss but rather to its increase because of electric resistance in the zones of poor electric contact.

The rest of the contact surface (subsequently referred to as the passive part) is acted upon mainly by the passive pressure p_p. The passive pressure and the length of the passive part of the contact surface L_p (Fig. 1), where the pressure acts, depend on the conditions of both armature and bore deformations under operating loads, and in every specific case can be determined from the solution of the contact problem for mechanically deformed solid bodies.

Considering all that is discussed above, relation (1.1) can be written in the following form:

$$N = N_a + N_p. \tag{1.2}$$

Here

$$N_a = r_0 \int_0^{2\pi} \int_0^L (p_a(\psi, z) + p_p(\psi, z))\, d\psi\, dz; \tag{1.3}$$

$$N_p = r_0 \int_0^{2\pi} \int_0^L p_p(\psi, z)\, d\psi\, dz. \tag{1.4}$$

This paper is not concerned with pressure forces in the electric contact zone, N_a, because correct calculations of three-dimensional electromagnetic fields are needed, which is a separate, rather complex problem. Subsequently, the force N_p that directly influences the energy loss due to friction is studied.

For the cylinder armature the contact pressure p_p is axially symmetric, and relation (1.4) takes the form

$$N_p = 2\pi r_0 \int_0^L p_p(z)\, dz.$$

The length of the passive part L_p can be determined using geometry:

$$L_p = L - L_a.$$

In the simplest case the length of the active part $L_a \approx L_s + \delta$, where L_s is the depth of the slot in the armature; δ is the average depth of a skin-layer for the acceleration time. Considering $L_s \gg \delta$ in most of the

TABLE 1

Armature type	Mass, g	L_s, mm	Diameter, mm	L_a, mm	L_p, mm
N_1	150	98	29.5	60	40*
N_2 (with payload)	320	180	29.6	58	122

Note: * denotes that the end neck is not included.

TABLE 2

Armature type	Maximum acceleration, m/sec2^2	Armature material characteristics		
		Elasticity modulus, GPa	Poisson's ratio	Density, g/cm^3
N_1	1400000	75.3	0.31	2.79
N_2	500000	75.3	0.31	2.79

practically important cases, when estimating the normal pressure force N_p, one can maintain $L_a \approx L_s$.

The relations obtained allow one to carry out a comparative analysis of possible energy loss due to friction during the electromagnetic acceleration of conductive armatures of various constructions and to formulate recommendations for improving these constructions in order to reduce the losses.

Let us make a comparative analysis of two cylinder armatures which are shown in Fig. 2 (all sizes are given in millimeters) and whose main characteristics are given in Table 1. The armatures are made of aluminum alloy. A payload of mass 87 g is placed in front of the armature N_2.

Calculations of contact pressure have been carried out using a finite-element calculating program based on the solution of the static axially symmetric contact problem of elasticity using the finite-element method, which made it possible to take into account the geometrical shape and peculiarities of the armature construction as well as the contact interaction between the armature and the surface of the railgun bore.

In the calculations the influence of electromagnetic forces on the moving armature was simulated by the action of mass forces applied to the armature which rested on its butt-end against an absolutely hard wall. The main initial data used in calculations of the contact pressure are given in Table 2.

The results of the calculations are shown in Fig. 3 in the form of curves of contact pressure distribution over the passive parts for two types of armature (curves 1 and 2 correspond to the armatures N_1 and N_2). Here the current length of the contact surface is plotted along the x axis with the origin coinciding with the leading edge of the contact on the head part of the armature. In such a coordinate system integral (1.4) is equal to the square of the flat figure enclosed by the contact pressure curve, x-axis, and a perpendicular dropped from the end of the pressure curve onto the x axis. The larger the square of the figure, the higher the force of the normal pressure and the higher are the frictional losses. Comparison of the squares enclosed by curves 1 and 2 shows that at maximum acceleration of the armature N_1 the energy loss by friction is 12.5 times less than it is at maximum acceleration of the armature N_2.

The length of the passive contact part of armature N_2, and thus the frictional losses, can be reduced by modification of its construction, particularly by grooving a wide circular neck in this part. Its dimensions essentially depend on length and mass of the armature, on the level of the load being applied to the armature during acceleration, on the difference between the diameters of the armature and the bore, and on the mechanical characteristics of the armature material. These dimensions must be chosen on the basis of the following main requirements which the neck has to satisfy: it should not disturb the stability of the armature in-bore motion; it must provide a guaranteed clearance between the armature and the bore along the whole acceleration distance; the neck shape must preclude any strain concentrations which would strongly influence the armature strength.

The neck grooved in the armature N_2 (Fig. 4, all sizes are given in millimetres) meets all the above-

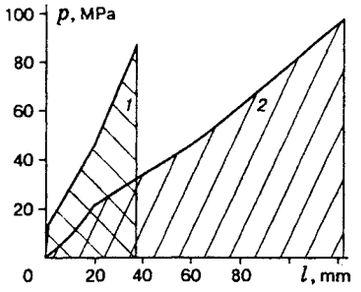

Fig. 3

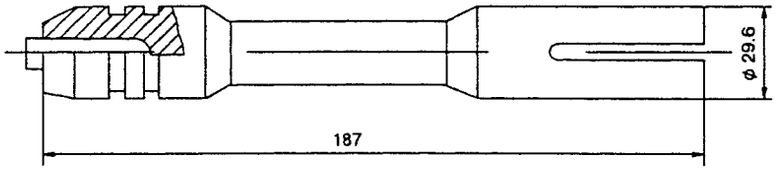

Fig. 4

listed requirements. The passive part of the contact is divided into two zones: the head zone providing stability of in-bore motion, and the tail zone ensuring a smooth pass to the active part of the contact.

The distribution of the contact pressure along the passive part of the contact surface for the armature N_2 with the neck is shown in Fig. 5 (curve 1). In this case, estimation of the normal pressure force shows that it is roughly two times greater than that in the case of the armature N_1 (see Fig. 2). So, it is expected that for the armature N_2 with the neck the frictional losses in the passive part of the contact will be sufficiently reduced.

The distribution of the radial movements over the armature neck is shown in Fig. 6. One can see that the maximum movement of the neck top does not exceed 8 μm. Consequently, this ensures clearance between the armature and the bore in the neck zone during acceleration.

The distribution of contact pressure for the armature with a neck, whose payload mass was increased to 267 g, is given in Fig. 5 (curve 2). The maximum acceleration of the armature was 440,000 m/sec^2. Estimation of the normal pressure force in this case shows it had increased roughly two times in comparison to that for the initial version of the armature. The maximum movement of the neck top increased up to 17 μm. However, the normal pressure force still remains 3–4 times less than that for the armature without a neck. This provides a basis for expecting a decrease of the frictional losses during the acceleration of the armature of type N_2 with a neck.

2. The main parameters of the experiments performed are given in Table 3. A capacitor bank with a total energy of about 5 MJ at a charge voltage 4.3 kV was used as a power source. The power source control system allowed a current impulse in the railgun to be formed by means of sequential firing of the bank modules at certain intervals which can be determined according to the condition of each experiment.

All the experiments have been carried out using the railgun MK which had the following characteristics: bore caliber 30 mm, bore length 4.2 m, rail material bronze, insulator material fiberglass. A powder gun was used as an injector. The following parameters were recorded in the experiments: current in the railgun circuit and in some circuits of bank modules, input (breech) and output (muzzle) voltage drops. The moments of the current-layer passage were measured by inductive probes placed along the railgun. The moments of projectile passage were registered by contact detectors in the outer path. Rapid filming of macroparticles in flight was also performed. A more detailed description of the installation is given in [3].

All the experiments can be divided into two groups: 1) those without any payload (Nos. 1–3), 2) those with a payload (Nos. 4–6). The experiments without payload have made it possible to select a construction

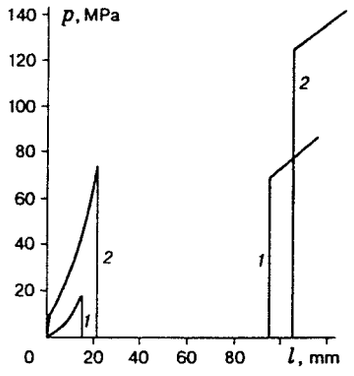

Fig. 5

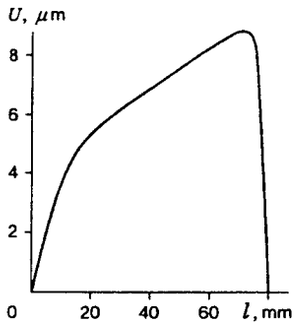

Fig. 6

TABLE 3

Shot No.	Macroparticle parameters				V_0	Output velocity	Stored energy	Θ^1	η^3_{RG}	η^4_{BC}
	Total mass	Load mass	L	L_s						
	g		mm		km/sec		MJ		%	
1	150.0	—	106	54	1.45	2.7	5.08	0.16	18.8	7.7
2	140.3	—	104	50	1.60	2.3	3.70	0.17	15.0	5.2
3	150.0	—	106	54	2.00	2.0	5.08	0.82	—	—
4[2]	320.0	87.0	167	51	1.05	1.6	5.08	0.50	—	3.6
5	327.0	107.0	190	37	1.05	1.5	5.08	0.50	10.0	3.7
6	305.4	84.2	159	43	1.10	1.6	5.08	0.43	11.2	5.6

Note:
(1) friction coefficient (total drop of Lorentz force due to friction);
(2) reliable record of the input voltage is missing;
(3) ratio of the increase in projectile kinetic energy in relation to the railgun (RG) power consumption;
(4) ratio of the increase in projectile kinetic energy in relation to the energy stored in capacitor batteries (BC).

of the current-carrying element of the macroparticle (the armature) that provided successively metallic, quasimetallic (microarc), and arc regimes of current flowing in the sliding contact. The contact was improved by means of forced pressing of the armature tail, where a longitudinal slackening slot was made.

In experiments Nos. 1 and 2 velocities of 2.1–2.7 km/sec were achieved; the armature construction was optimized at currents up to 1240 kA, which enabled experiments with payload and with total macroparticle mass more than 300 g to be performed. In experiments Nos. 4 and 5 macroparticles whose design is shown in Fig. 2b were used.

Analysis of the experiments performed has shown that the friction increased sharply as the contact pressure increased when there was no acceleration by the electromagnetic force. The electromagnetic force decrease due to friction was more than 50%.

The macroparticle construction was improved according to the above-discussed considerations. Shortening of the sliding surface by grooving a neck enabled the friction force to be decreased (the friction coefficient dropped to 0.43) and in-bore velocity to be increased. This indicates that the main processes which take place during projectile acceleration in a railgun are correctly understood.

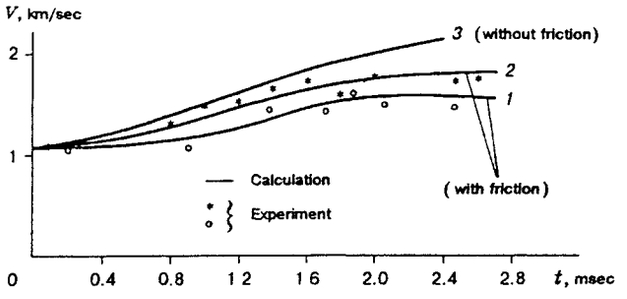

Fig. 7

Comparison of the two functions $V(t)$ for macroparticles with and without a neck (curves 1 and 2) is given in Fig. 7. Calculational results for the ideal case without friction are also shown (curve 3).

Thus, a model was created which made contact pessure calculations possible. A comparative analysis for two cylindrical U-shaped armatures has been carried out (armature N_1 without load, and N_2 with payload in the head part of the armature). It has been shown that frictional losses of the armature of type N_2 could be sufficiently reduced by grooving a wide circular neck in the passive part of the armature.

For further results it is necessary to have more correct accounting of the balance between the forces which provide pressing of the armature tail, necessary for arcless electric current conditions in the contact, and the normal pressure forces, which influence the friction. To achieve this, the three-dimensional problem of nonstationary electromagnetic, thermal, and force field distribution over the zone of moving contact must be solved.

REFERENCES

1. B. A. Urykov, A. D. Lebedev, and C. C. Milyaev, "Influence of materials' properties on the dynamics of metal armature acceleration in a railgun," Proc. 4th Eur. Symp. on Electromagnetic Launch Technology, May 2–6, 1993, Celle, Germany, p. 1022.
2. Czu Hsiung Chu, "A simple theoretical model for projectile in bore motion of electromagnetic railguns," Proc. 5th U. S. Army Symp. on Gun-Dynamics, Sept. 23–25, 1987, pp. 204–232.
3. Yu. P. Babakov, A. V. Plekhanov, and V. B. Zheleznyi, "Range and railgun results at LS and PA 'Soyuz'," *IEEE Trans. Magn.*, **31**, No. 1, 259–262 (1995).